Role of Cu^{2+} as an Additive in an Electroless Nickel−Phosphorus Plating System: A Stabilizer or a Codeposit?

Chun-Han Chen,[†] Bing-Hung Chen,*[,†,‡] and L. Hong[§]

Department of Chemical Engineering and Center for Micro/Nano Science and Technology, National Cheng Kung University, 1 University Road, Tainan 70101, Taiwan, and Department of Chemical and Biomolecular Engineering, National University of Singapore, 4 Engineering Drive 4, Singapore 117576

Received December 13, 2005. Revised Manuscript Received March 2, 2006

The effect of cupric (Cu^{2+}) ion as an additive in the acidic electroless nickel plating (ENP) bath on the characteristics of the resulting nickel−phosphorus (Ni−P) alloys was investigated mainly with X-ray diffraction, scanning electron microscopy, and energy-dispersive X-ray (EDX) spectrometry. Cupric ions in the acidic ENP bath using hypophosphite anions as reductants have been reported ambiguously as stabilizers or codeposit constituents. In this work, the critical concentration of added copper salts, $CuSO_4 \cdot 5H_2O$, that starts to inhibit the ENP process was determined to be ca. 536 mg/L. In general, the deposition rate, surface morphology, and pit formation on the surface of as-deposits are significantly improved with Cu^{2+} addition at concentrations less than the critical value. The electroless nickel alloys were shown as a mixture of an amorphous deposit and a crystalline copper metal rather than as amorphous alloys alone.[1,2] During the initial stage of the electroless plating process, the copper contents in as-deposits were found to decrease rapidly with plating time from the EDX analyses. The X-ray photoelectron spectroscopy result also confirms that copper is the preferred deposited species during the initial stage of the ENP process. The theoretical model[3] is revised by taking into account the effect of adsorbed cupric ions on the shift in the depth of the net nuclear potential of the electroless nickel frontier, and successfully predicts the deposition rates. Moreover, as predicted by the revised model, the adsorbed cupric ions on the just-deposited Ni−Cu−P frontier could enhance the adsorption of hypophosphite anions and, accordingly, the deposition rates.

1. Introduction

Over the years, the electroless nickel plating (ENP) technique has experienced a rapidly increasing demand in a broad spectrum of industrial practices,[4−11] development in nanotechnology recently,[12−14] etc. In an ENP process, the nickel ions are generally reduced on conductive surfaces, commonly the just-deposited nickel frontier, in the presence of chemical reducing agents, in place of an external electric current.[4] In the ENP process, an acidic ENP bath containing hypophosphite ions ($H_2PO_2^-$) as reducing agents is most frequently used, in which the overall reaction could be expressed as[3,4]

$$Ni^{2+} + 2H_2PO_2^- + 2H_2O \xrightarrow{\text{cat.}} Ni^0 + 2H_2PO_3^- + 2H^+ + H_2 \quad (1)$$

In other words, the ENP process is a redox reaction with continued deposition of nickel on the substrate through the catalytic action of the deposit itself.[4] The electrons are released through the anodic reaction between hypophosphite ions and water on conductive substrates. In addition to the cathodic reduction of nickel ions, hypophosphite ions can also be reduced to phosphorus element in the presence of hydrogen ions[3] (Figure 1). The extents of the cathodic reactions of both nickel ions and hypophosphite ions will contribute to the compositions of the resulting electroless nickel (EN) deposits. If the weight contents of the phosphorus exceed approximately 7−8%, the resulting Ni−P alloy is amorphous, which accounts for the majority of industrial applications of such alloys.[4,15] Additionally, evolution of H_2

* To whom correspondence should be addressed. Phone: +886-6-275-7575 ext 62695. Fax: +886-6-234-4496. E-mail address: bhchen@alumni.rice.edu.
[†] Department of Chemical Engineering, National Cheng Kung University.
[‡] Center for Micro/Nano Science and Technology, National Cheng Kung University.
[§] National University of Singapore.

(1) Armyanov, S.; Georgieva, J.; Tachev, D.; Valova, E.; Nyagolova, N.; Mehta, S.; Leibman, D.; Ruffini, A. *Electrochem. Solid-State Lett.* **1999**, *2*, 323.
(2) Valva, E.; Dille, J.; Armyanov, S.; Georgieva, J.; Tatchev, D.; Marinov, M.; Delplancke, J.-L.; Steenhaunt, O.; Hubin, A. *Surf. Coat. Technol.* **2005**, *190*, 336.
(3) Yin, X.; Hong, L.; Chen, B.-H. *J. Phys. Chem. B* **2004**, *108*, 10919.
(4) Mallory, G. O.; Hajdu, J. B. *Electroless Plating: Fundamentals and Applications*; American Electroplaters and Surface Finish Society: Orlando, FL, 1990.
(5) Yamauchi, Y.; Yokoshima, T.; Momma, T.; Osaka, T.; Kuroda, K. *J. Mater. Chem.* **2004**, *14*, 2935.
(6) Chen, S. T.; Chen, G. S. *J. Electrochem. Soc.* **2004**, *151*, D99.
(7) Balaraju, J. N.; Rajam, K. S. *Surf. Coat. Technol.* **2005**, *195*, 154.
(8) Chen, C.-J.; Lin, K.-L. *J. Electrochem. Soc.* **1999**, *146*, 137.
(9) Xu, H. W.; Brito, J.; Sadik, O. A. *J. Electrochem. Soc.* **2003**, *150*, C816.
(10) Xu, Q.; Zhang, L,; Zhu, J. *J. Phys. Chem. B* **2003**, *107*, 8293.
(11) Brown, R. J. C.; Brewer, P. J.; Milton, M. J. T. *J. Mater. Chem.* **2002**, *12*, 2749.
(12) Wang, T. C.; Rubner, M. F.; Cohen, R. E. *Chem. Mater.* **2003**, *15*, 299.
(13) Zhang, Z. T.; Dai, S.; Blom, D. A.; Shen, J. *Chem. Mater.* **2002**, *14*, 965.
(14) Tai, Y. L.; Teng, H. S. *Chem. Mater.* **2004**, *16*, 338.
(15) Abrantes, L. M.; Fundo, A.; Jin, G. *J. Mater. Chem.* **2001**, *11*, 200.

10.1021/cm0527571 CCC: $33.50
Published on Web 06/06/2006

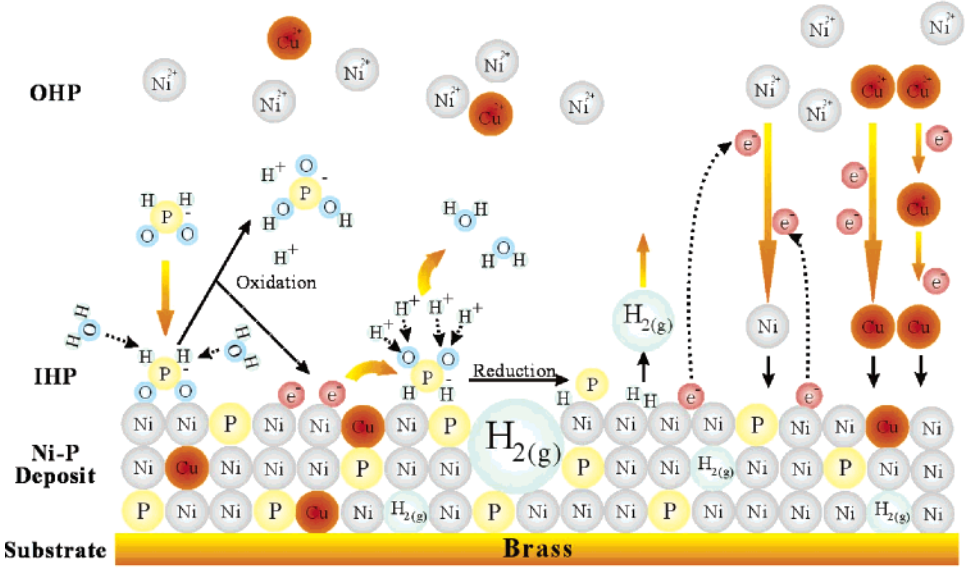

Figure 1. Schematic illustrating two different reaction pathways through which hypophosphite ions are converted to orthophosphate and phosphorus and Ni−Cu−P alloys are deposited.

gas bubbles absorbed on the EN deposits inevitably leaves voids on as-deposits and causes great concerns about the corrosion-resistive properties of the deposits, in which the deposits are prone to pit corrosion.[16] Consequently, wetting agents have to be included in the ENP formulation to reduce the $H_{2(g)}$ adsorption and the associated formation of voids.[3,4,16]

As aforementioned, the ENP process is indeed a redox reaction in solution and could continue by itself, once it is initiated. That is, the ENP bath is chemically metastable. Hence, complexing agents[17] and stabilizers are always included in the ENP bath to prevent it from happening with the unwanted precipitation of nickel ions in the solution. Regrettably, deposition rates are consequently reduced, and the properties of the resulting Ni−P alloys are altered accordingly. The concentrations of the bath stabilizers could be as low as only a few parts per million, which poses a great challenge to us in finding successful ENP formulations. Consequently, proper deposition conditions and ENP formulations require our great attention.

The complicated nature of the ENP process has not been fully understood, though many works have been devotedly studied.[1,3,11−19] In particular, the stabilizing mechanism in the ENP process has not received much attention yet.[3,4] The main function of stabilizers in the ENP bath is to avert the heterogeneous reaction in the bath solution that triggers the subsequent random decomposition of the entire plating bath.[4]

The stabilizer plays a mysterious role in the ENP process. A trace amount of heavy metal ions, for instance, Pb^{2+} as a very common stabilizer, keeps the plating bath free of propagation of colloidal nickel particles, which eventually lead to catastrophic precipitation of nickel blacks in the plating bath.[4,19] Yin et al.[3] have attempted to solve this riddle by combining the knowledge of the electrical double layer and the quantum tunneling theory of an electron from the Fermi level of the Ni−P plating frontier to Ni^{2+} ions located at the outer Helmholtz plane. They have arrived at a nice prediction about the effect of Pb^{2+} stabilizers on the compositions and deposition rates of the resulting Ni−P alloys. However, the operation window of using Pb^{2+} stabilizers is quite narrow and less than 12.5 ppm, so its distribution in the resulting Ni−P deposits may not be easily and precisely determined.[3] Moreover, lead ions in excess could give fatal damage to the brain and nerves. Consequently, a lead-free process has been encouraged; for example, the European Union has imposed the RoHS directive to restrict the use of lead.

To further validate the prediction proposed by Yin et al.,[3] cupric Cu^{2+} ions are selected as a model stabilizer for replacing lead ions in the acidic ENP formulations and for studying the effect of the stabilizer concentration on the characteristics of the electroless nickel alloys. The choice of cuprous ions is mainly based on the facts that (1) cuprous and cupric ions have been reported with stabilizing functions,[1,18] (2) they provide a wider concentration window than lead ions for operation, and (3) superior characteristics of electroless nickel deposits are obtained with a codeposit of copper.[9]

Armyanov et al.[1,7,18] have observed an increasing deposition rate and reduced pit formation on the Ni−P alloys plated from the acidic ENP bath with addition of Cu^{2+}. They have obtained high phosphorus Ni−Cu−P coatings containing ~3 wt % copper from the acidic ENP bath with 14−16 ppm Cu^{2+} added, or equivalently, 55−62 mg/L $CuSO_4 \cdot 5H_2O$. Subsequently, they have attempted to obtain the optimal conditions for depositing the electroless Ni−Cu−P coatings.[18] The smoothness, brightness, ductility, corrosion resistance, and thermal stability of the electroless Ni−P (12 wt %) deposit have been found to increase enormously when the codeposited copper is ca. 1 wt %.[1,7,18] Interestingly, Chen and Lin[8] have reported that excess $CuSO_4$ added in the

(16) Chen, B.-H.; Hong, L.; Ma, Y.;. Ko, T.-M. *Ind. Eng. Chem. Res.* **2002**, *41*, 2668.
(17) Cui, G. F.; Li, N.; Li, D. Y.; Chi, M. L. *J. Electrochem. Soc.* **2005**, *152*, C669.
(18) Georgieva, J.; Armyanov, S. *J. Electrochem. Soc.* **2003**, *150*, C760.
(19) Yin, X.; Hong, L.; Chen, B.-H.; Ko, T.-M. *J. Colloid Interface Sci.* **2003**, *262*, 89.

Table 1: Composition of the Plating Bath Used in This Work

chemicals	concentration
$NiSO_4 \cdot 7H_2O$	26 g/L
$CH_3COONa \cdot 3H_2O$	16 g/L
$NaH_2PO_2 \cdot H_2O$	38 g/L
sodium citrate	46 g/L
$CuSO_4 \cdot 5H_2O$	variable
pH	4.8 ± 0.1
temperature	90 ± 1 °C

plating bath could impede the formation of the amorphous Ni−P alloys in a slightly basic ENP bath.

In this work, the effect of cupric ion as an additive in the acidic ENP bath using hypophosphite anions as reductants on the characteristics of the resulting Ni−P alloys was investigated. Copper ions not only act as a stabilizer and an accelerator in the electroless Ni−P deposition, but are also found to compete with nickel ions in the metal reduction from this work. Careful experiments emphasizing the initial deposition process were conducted and replicated 50 times under the same plating condition to give distinguishable X-ray diffraction (XRD) patterns, indicating that metallic copper with preferred facet (1,1,1) of up to 5 wt % is initially deposited alone, rather than as a Ni−Cu−P alloy. Moreover, the Ni/P elemental ratio is observed to not be affected by the addition of copper sulfate pentahydrate, up to the critical concentration of ca. 536 mg/L, to the ENP bath. More detailed results and discussion are summarized in this paper.

2. Experimental Details

2.1. Substrates and Reagents. ENP was conducted on brass substrates ($20 \times 10 \times 0.17$ mm) with acidic formulation (Table 1). For convenience, the composition of each ingredient is given in the total weight of salt added to the plating bath. The brass substrates were first cleaned with a soak cleaner in an ultrasonic bath for 20 min, followed by removal of surface oxides in a H_2SO_4 solution (10 vol %) for 3 min at ambient temperature. Pure brass cannot be electrolessly plated by nickel. Consequently, tiny Pd particles were introduced to the brass surface as the seeds for initiating the catalytic reduction of Ni by immersing brass substrates into 0.1 M $SnCl_{2(2\ M\ HCl)}$ and 0.05 M $PdCl_{2(2\ M\ HCl)}$ for 6 and 2 min, respectively. Between each step, brass substrates were rinsed with deionized water for 20 s. In the final step, the brass substrate was rinsed with deionized water twice and blow-dried with nitrogen.

Moreover, gold substrates were employed in experiments focusing on the effect of cupric ions on the initial deposition of the ENP process. These substrates consist of Au(100 nm)/Ti(10 nm)/glass substrates from the PVD technique. Zinc is used to initiate the deposition process.

Reagent grade chemicals used in the ENP formulations were purchased from Riedel-de Haën. These chemicals include nickel-(II) sulfate heptahydrate, sodium acetate trihydrate, sodium hypophosphite monohydrate, sodium citrate, cupric sulfate pentahydrate, and ammonium hydroxide solution. All chemicals are used as received. The compositions of the plating baths and plating conditions are given in Table 1. Deionized water from a Millipore Milli-Q system having a resistivity greater than 18.2 MΩ·cm was used in the sample preparations.

2.2. Characterization of Deposited EN Alloys. The compositions of the deposited alloys on the brass substrates were determined using an Oxford energy-dispersive X-ray (EDX) spectrometer installed on a Hitachi S4100 field emission scanning electron microscope and a JEOL JSM-6700F. Both scanning electron microscopes were employed to observe the surface morphology of the deposits as well. The initial beam energy used in the EDX and scanning electron microscopy (SEM) analyses was 10 and 15 kV. With information given by the manufacturer, the depth of penetration for the electron beam is estimated at ca. 200 nm under the experimental conditions used in this work. Furthermore, depth profiles of the compositions of selected samples were examined with an X-ray photoelectron spectrometer, model VG ESCALAB 250, equipped with an Al Kα X-ray source (at 1486.6 eV). The structures of the deposited EN alloys were analyzed with a Rigaku RINT 2000 X-ray diffractometer using a Cu Kα X-ray as the radiation source. The existence of colloidal particles harvested from plating baths was confirmed with a Hitachi HF-2000 transmission electron microscope.

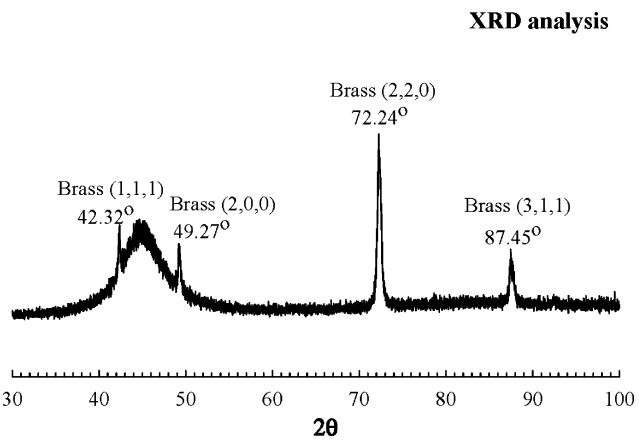

Figure 2. XRD pattern of an electroless Ni−P alloy (plating time 0.5 h, no stabilizer).

ENP was conducted by immersing brass substrates into ENP solutions (Table 1). The plating rate (R) [mg/(cm²·h)] was determined with the gravimetrical method and calculated according to the following formula:

$$R = \frac{(M_t - M_0) \times 60}{A_s t} \tag{2}$$

where t is the plating duration (min), M_t the mass (mg) of the object plated for a period of time t, M_0 the initial mass (mg) of the substrate, and A_s the exposed surface area (cm²) of the specimen. The plating load was fixed at 40 cm²/L. The deposition rates of phosphorus (R_P), nickel (R_{Ni}), and copper (R_{Cu}) were calculated, respectively, as follows:

$$R_P = R[\mathrm{P}] \tag{3}$$

$$R_{Ni} = R[\mathrm{Ni}] \tag{4}$$

$$R_{Cu} = R[\mathrm{Cu}] \tag{5}$$

where [P], [Ni], and [Cu] are the contents (%) of phosphorus, nickel, and copper by mass in the EN alloys.

3. Results

The characteristics of the electroless nickel alloys were mainly examined with XRD, SEM, and EDX analysis. Figure 2 shows a typical amorphous morphology of the Ni−P deposit plated for 30 min from the higher phosphorus content ENP acidic formulation without addition of any Cu^{2+} ion. This results in the Ni−P deposit having about 12 wt % phosphorus. A broad peak centered at $2\theta = 44.8°$ indicates

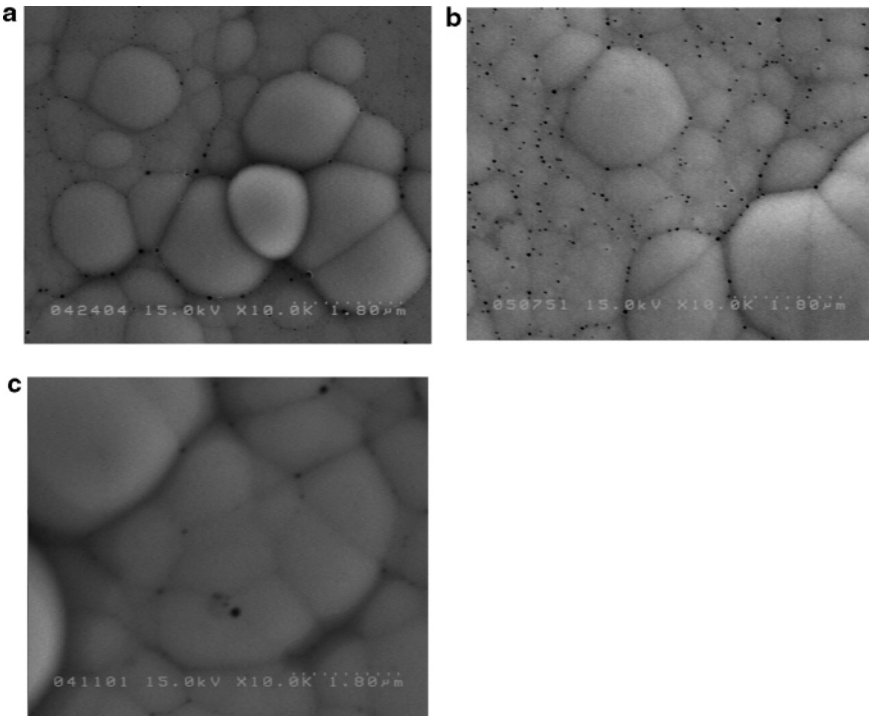

Figure 3. Effect of stabilizers on the surface morphology of electroless nickel alloys: (a) no stabilizer added, plating time 20 min; (b) [Pb·$(CH_3COO)_2$] = 1 mg/L, time 30 min; (c) [$CuSO_4$·$5H_2O$] = 100 mg/L, plating time 30 min.

the amorphous nature of the deposits, which is consistent with the knowledge that the EN alloys become amorphous when their [P] is above 7−8 wt %.[4,15]

The SEM micrograph clearly shows the formation of pits, ranging from a few nanometers to 100 nm, on the surface of as-deposits plated with/without stabilizers (Figure 3). The Ni−P deposits plated from the ENP bath with 1 ppm lead acetate added, a conventional stabilizer widely used in ENP baths, or without any stabilizer added have exhibited densely populated pits having dimensions of less than 80 nm. Lead ions are quite effective stabilizers, posting a critical concentration near 12.5 ppm.[3] However, lead ions cannot reduce the formation of voids. In contrast, diminishing pits are seen on the Ni−P alloy deposited from the ENP bath with $CuSO_4$·$5H_2O$ added at a concentration less than the critical value.

These voids are believed to arise from the adsorbed H_2 bubbles on EN alloys that block subsequent deposition of EN alloys on these occupied sites (Figure 1). With these pits, the anticorrosion property of EN alloys would have been deteriorated.[16] Thus, a diminishing pit formation is warranted, which is achievable with Cu^{2+} addition at concentrations less than the critical value.

The effects of the $CuSO_4$ concentration added in the ENP bath on the average deposition rates of EN alloys are presented in Figure 4, which shows a critical concentration of ca. 536 ppm, where stabilizers not only prevent the plating bath from collapsing, but also start to slow the deposition process beyond the critical concentration. At concentrations less than the critical value, the deposition rates are not influenced by the presence of stabilizers. The resulting deposition rate is 5.7 (mg·cm^2)/h, or 7.4 μm/h using an estimated density of deposit equal to 7.8 g/cm^3.[4] However, when $CuSO_4$ is added in excess, the plating process is retarded and the nature of the electroless nickel plating is

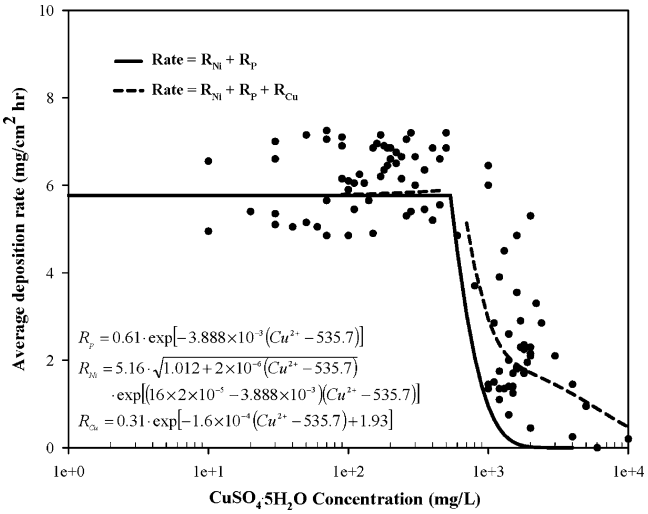

Figure 4. Effect of the $CuSO_4$·$5H_2O$ concentration in the plating bath on the average deposition rates of Ni−P alloys (plating duration 0.5 h).

changed. In this regime, the model proposed by Yin et al.[3] fails to predict the empirical deposition rate, unless the codeposition of copper onto the electroless Ni−P alloy has been duly considered.

To further investigate the effect of added $CuSO_4$ in the plating bath on the compositions of the resulting EN alloys, the concentration of $CuSO_4$ in the plating bath is set not to exceed the critical value. Figure 5 clearly shows that the copper contents in the electroless nickel deposits plated for 30 min increase gradually to ca. 5 wt % when the initial $CuSO_4$·$5H_2O$ concentration is greater than 150 mg/L. Coincidently, the copper contents in the deposits plated for 30 min could be well fit with an exponential function of the $CuSO_4$ additive concentration in the bulk.

In contrast, the P contents decrease slightly from 11.6 to 10.4 wt % and the Ni contents drop from 87 to 83 wt %,

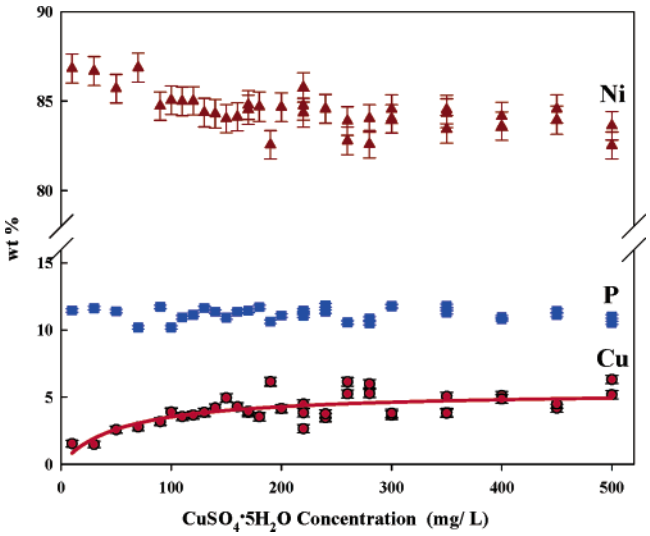

Figure 5. Effect of the $CuSO_4 \cdot 5H_2O$ concentration in the plating bath on the composition of the resulting Ni−P deposits (0.5 h plating duration).

which indicates that the electroless nickel alloys obtained in this work are of high phosphorus contents.[4,15] However, the Ni/P mass ratios in the deposits remain fairly constant at 8 for an added $CuSO_4 \cdot 5H_2O$ concentration increased to 500 mg/L. That is, the constituent ratio of Ni/P by mass in the alloys is not affected by the appearance of copper.

It is noteworthy that the average thickness of the deposited film plated for 30 min is 3.7 μm and the penetration depth of the electron beam used in EDX is around 200 nm. Consequently, the results reported in Figure 5 are the enveloped average of the regime from the surface to that at 200 nm depth or, equivalently, the layer corresponding to the plating time from 28 to 30 min.

The Ni/Cu atomic ratios in the deposits plated for 30 min decrease progressively from 40 to 19 when the initial $CuSO_4 \cdot 5H_2O$ concentration increases from 50 to 500 mg/L. In the meantime, the Ni^{2+}/Cu^{2+} molar ratio in the bulk solution varies from 462 to 46.2. This indicates that copper ions present in plating baths possess a greater tendency to be reduced into electroless metal deposits than nickel ions.

Alternatively, the effect of added $CuSO_4$ on the characteristics of EN alloys has been studied as well beyond the critical concentration. Figure 6a exhibits the XRD patterns of deposits plated for 30 min and 3 h from the ENP bath with an initial addition of 1000 mg/L $CuSO_4 \cdot 5H_2O$. The XRD pattern corresponding to that plated for 30 min has clearly shown the characteristic peaks of the brass substrate, and one in line with Cu(1,1,1), $2\theta = 43.32°$, as well as the broadened peaks of amorphous Ni−P alloys ($2\theta = 38-54°$). Similarly, with the deposit plated for 3 h, the peaks associated with the brass substrate almost disappear, but the one resulting from Cu(1,1,1) is still discernible. Interestingly, the characteristic peak of Cu(1,1,1) is not very prominent on the EN deposits plated from the bath with 100 ppm $CuSO_4 \cdot 5H_2O$ added, which will be presented later in Figure 10 and discussed later in the text.

The corresponding SEM pictures clearly show piles of grains, with sizes near 500 nm, on the substrates for those plated for 30 min and slumps with pits near 150 nm on the

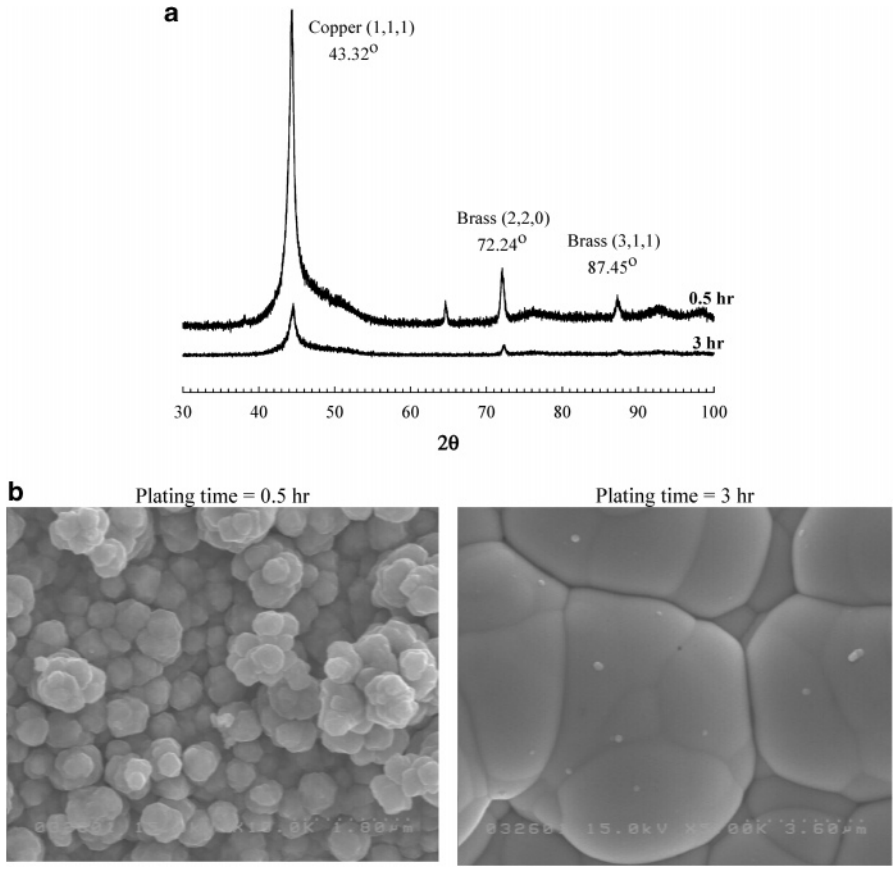

Figure 6. XRD pattern and SEM micrographs of an electroless Ni−P alloy (plating time 0.5 and 3 h, $[CuSO_4 \cdot 5H_2O] = 1000$ mg/L): (a) XRD pattern, (b) SEM micrographs.

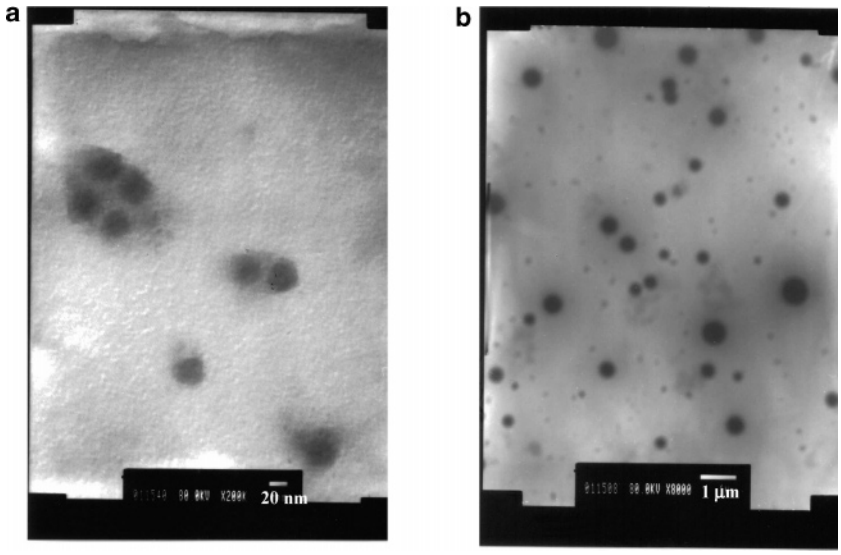

Figure 7. TEM photos of colloidal particles harvested from the plating bath after being plated for 0.5 h: (a) [$CuSO_4 \cdot 5H_2O$] = 100 mg/L, scale bar 20 nm; (b) [$CuSO_4 \cdot 5H_2O$] = 1000 mg/L, scale bar 1 μm.

substrates from those plated for 3 h. The EDX analyses reveal the average copper content in the samples plated for 30 min is around 90 wt %. In addition, the deposits plated with more than 3000 mg/L $CuSO_4 \cdot 5H_2O$ added do not contain nickel or phosphorus anymore. Only copper is found. The deposits look dark pink or purple, which is consistent with the color of copper.

According to Yin et al.'s study on the stability mechanism of the ENP bath,[19] the detachment of colloidal Ni particles from the plating frontier and their reentrance to the bulk solution cause the rapid growth of nickel flakes in the plating bath, as these Ni colloidal particles become parent nuclei for subsequent EN deposition in the bulk. Consequently, the nickel black is produced suddenly and the plating bath is no longer available for the ENP process. One function of stabilizers is to occupy the catalytic sites on these tiny nickel particles or to saturate the coordination-unsaturated nickel nuclei.[19] Figure 7 shows TEM photographs of colloidal particles harvested from plating baths with addition of 100 and 1000 ppm $CuSO_4 \cdot 5H_2O$ after a 30 min plating process. With 100 ppm $CuSO_4 \cdot 5H_2O$ added, the dimensions of these particles are less than 25 nm, in contrast with those with sizes as large as 600 nm from the plating bath with 1000 ppm $CuSO_4 \cdot 5H_2O$ added. ICP-MS analyses on the metal components of these large particles dissolved in nitric acid yield a mass ratio of Cu/Ni close to 65/35. This peaks our interest in the question of whether copper is deposited preferentially over nickel during the initial stage of the ENP process.

A series of experiments were conducted by varying the plating time of EN alloys in the ENP bath with the $CuSO_4 \cdot 5H_2O$ concentration fixed at 100 mg/L. Under this condition, the deposition rate is 5.7 (mg·cm^2)/h or, equivalently, 7.4 μm/h and 123 nm/min. The analysis depth of EDX used in this work is approximately 200 nm. As aforementioned, the results presented here are the enveloped average of a thin layer 200 nm thick. The copper contents for the plated samples with very a short plating time have been corrected with the contents of zinc resulting from brass substrates, since

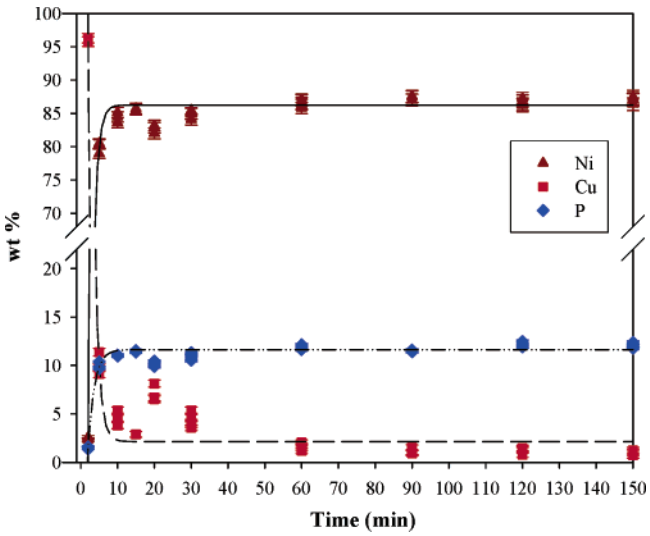

Figure 8. Effect of the plating time on the constituent distribution of an electroless nickel deposit ([$CuSO_4 \cdot 5H_2O$] = 100 mg/L).

the brass substrates used consist of 64 wt % Cu and 36 wt % Zn.

The amounts of nickel and phosphorus increase to constant values near 10 min after initiation of the ENP process (Figure 8). Simultaneously, the copper drops rapidly with the plating time. The first two data points in Figure 8 report the measurements on deposits taken away from the plating bath 2 and 5 min after initiation of the ENP process. The first sample contains 35.2 ± 0.3 wt % Pd and 3.8 ± 0.3 wt % Zn, whereas the second has 3.3 ± 1.3 wt % Pd and 0.7 ± 0.3 wt % Zn. The detailed contents of the first two samples reported in Figure 8 have been duly corrected by excluding the Pd content and the copper contribution from the substrates. This indicates the copper contents in the deposits decrease from 96 wt % at 2 min to 9 wt % at 5 min and 4.5 wt % at 4.5 min. In the meantime, the nickel contents increase from 2.5 to 80 and 84.5 wt %, respectively. This confirms that copper is preferably deposited during the initial stage of the plating process. In addition, SEM micrographs

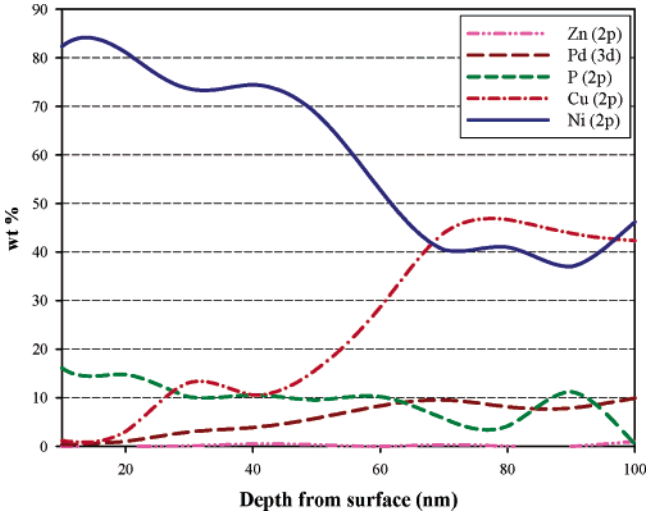

Figure 9. Concentration−depth profile of an electroless Ni−P alloy (plating time 3.5 min, [$CuSO_4 \cdot 5H_2O$] = 100 mg/L).

of both samples show that substrates are completely occupied with grains, presumably Pd and Cu particles.

To validate the findings on the time-dependent profile of the components analyzed by EDX, the sample plated for 3.5 min in Figure 9 was examined with X-ray photoelectron spectroscopy (XPS) on depth profiles of constituents in the deposits. These plating times give the thickness of deposits at about 430 nm and 3.7 μm. The XPS results on that plated for 30 min from the same conditions simply show the existence of Ni and P in the layer from the surface to 100 nm deep. The Ni content is close to 83 ± 2 wt %. However, the one corresponding to that for 3.5 min gives the presence of Ni, Cu, P, and Pd in the thin layer of 100 nm from the surface. Figure 9 further confirms that the copper and palladium contents in the analyzed layer increase with increasing depth from the surface.

Finally, a series of experiments were conducted deliberately under the same conditions but on Au(100 nm)/Ti(10 nm)/glass substrates, noted as Au substrate, made via the PVD technique. The substrates were immersed into the plating bath maintained at 90 °C for 15 s. The plating process was first initiated with zinc. Subsequently, the as-deposits were removed and plated in another pristine ENP bath under the same conditions. Such a process was repeated 50 times to amplify the existence of characteristic peaks associated with any possible crystal structure of Cu resulting during the initial plating process.

Three different samples under these operation procedures were scanned with XRD. The XRD instrument was set with a very small increment of 2θ at 0.01° from 30° to 90°. The results are summarized in Figure 10 and noted as "short time". For comparison, the XRD patterns of the Au substrate and Ni−P alloys plated for 10 and 30 min under the same conditions on the same Au substrates are presented in Figure 10 as well. The inset of Figure 10 clearly shows the existence of Cu(1,1,1) at 2θ = 43.32°. The noise of the baseline in Figure 10 is less than 8 counts per second (cps), an arbitrary unit used in XRD. In contrast, the height of the Cu(1,1,1) peak from the mean of the baseline is 20 cps, which is

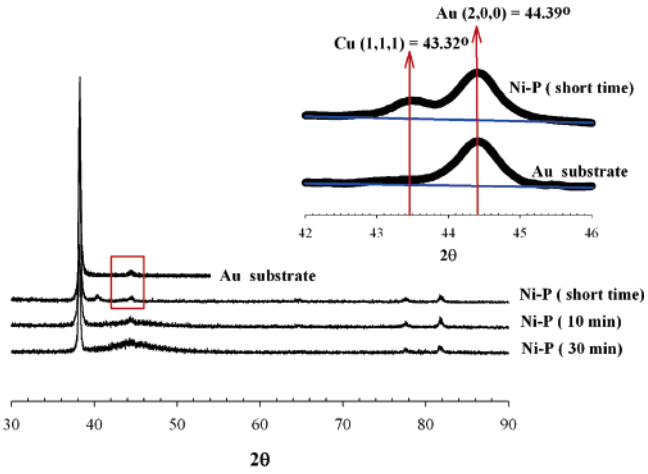

Figure 10. Effect of the plating time on the XRD patterns of Ni−P deposits ([$CuSO_4 \cdot 5H_2O$] = 100 mg/L, substrate Au(100 nm)/Ti(10 nm) on glass).

statistically significant enough to yield the existence of such a peak.

It has to be mentioned that such a prominent peak of Cu-(1,1,1) is not observed on the as-deposit with addition of $CuSO_4$ at a concentration less than the critical value. However, it is still possible that such peaks exist but are covered by the broad peak of Ni−P. In contrast, if the added $CuSO_4$ concentration exceeds the critical concentration, peaks associated with pure copper could be observed clearly on the as-deposits plated for 0.5 and 3 h (Figure 6).

According to the Sherrer formula, the effective grain size of Cu(1,1,1) is near 11.3 nm. Moreover, the electroless nickel alloy is not plated immediately after the onset of the plating process. This also signifies that, even at a concentration less than the critical concentration, copper is the predominant species to be plated. The preferential orientation of electroless copper is in the (1,1,1) direction.

4. Discussion

Addition of cupric ions to the ENP bath not only affects the deposition rate, but also improves the surface morphology of the resulting Ni−P alloy. Copper ions play a complicated role in the electroless deposition both as a stabilizer and as an electron scavenger against the nickel ions. In terms of a stabilizing effect, the presence of copper ions does not suppress the deposition rates significantly, unless the initially added $CuSO_4 \cdot 5H_2O$ concentration exceeds the critical value, i.e., 536 ppm. Concurrently, the plating bath with 100 mg/L $CuSO_4 \cdot 5H_2O$ added stored at 25 °C for two weeks shows no sign of solution decomposition, and still can be used in the plating experiment without any adverse effects. Furthermore, the same plating bath maintained at 90 °C could exist stably for more than 8 h.

The stabilizing effect of added cupric ions could be observed from the harvested colloidal particles shown in Figure 7. Addition of 100 mg/L $CuSO_4 \cdot 5H_2O$ successfully blocks propagation and growth of colloidal metal particles in the bulk plating bath. The larger particles found have diameters near 25 nm only. In contrast, growth of nickel was found on metal particles of ca. 600 nm collected from the ENP bath with 1000 mg/L $CuSO_4 \cdot 5H_2O$ initially added.

These particles contain nickel and copper in a 35/65 elemental ratio. They are likely colloidal copper grains, originally detached from the plating frontier, deposited with the electroless Ni−P alloy.

It is well-known that solutions for electroless copper plating are less stable than those of electroless Ni−P plating.[1] From an electrochemical point of view, copper ions have a greater preference to be deposited on the plating frontier than nickel ions do. This can be attributable to the much greater reduction potential of cupric ions than nickel ions, shown as the following equations:[4,21]

$$Ni^{2+} + 2e^- \rightarrow Ni \; [E_{25°C}{}^0(\text{NHE}) = -0.257 \text{ V}] \quad (6)$$

$$Cu^{2+} + 2e^- \rightarrow Cu \; [E_{25°C}{}^0(\text{NHE}) = 0.340 \text{ V}] \quad (7)$$

$$Cu^{+2} + e^- \xrightarrow{E_{25°C}{}^0(\text{NHE}) = 0.159 \text{ V}} Cu^+ + e^- \xrightarrow{E_{25°C}{}^0(\text{NHE}) = 0.52 \text{ V}} Cu \quad (8)$$

Combining both half-reactions of nickel and copper, the competition between the reductions of nickel and copper ions could be easily conceived from the constructed reaction of the redox couple expressed as

$$Cu + Ni^{2+} \rightarrow Cu^{2+} + Ni \; [E_{25°C}{}^0(\text{NHE}) = -0.597 \text{ V}] \quad (9)$$

where the equilibrium constant, K_{rxn}, can be rewritten as

$$K_{rxn} = \frac{[Cu^{+2}]_{solution}[Ni]_{solid}}{[Cu]_{solid}[Ni^{+2}]_{solution}} \equiv \frac{([Ni]/[Cu])_{deposit}}{([Ni^{+2}]/[Cu^{+2}])_{solution}} \quad (10)$$

The equilibrium constant of this reaction, K_{rxn}, is estimated to be around 6.6×10^{-21} at 25 °C and 2.7×10^{-17} at 90 °C from the Nernst equation.[21] However, in this work, the empirical value of K_{rxn} increases from 0.0865 to 0.411 after plating for 30 min, when the initial $CuSO_4 \cdot 5H_2O$ concentration increases from 50 to 500 mg/L, slightly less than the critical value. With K_{rxn} smaller than unity, a preferential deposition of copper will be observed. Alternatively, in view of the effect of the plating time on the equilibrium constants, data from Figure 8 were analyzed. K_{rxn} increases from 1.12×10^{-4} at 2 min to 0.03845 and 0.0812 at 5 and 10 min, respectively. Nonetheless, the obtained equilibrium constant is still much greater than the predicted value.

The main discrepancy mainly arises from the fact that metal copper cannot catalyze the oxidation of the adsorbed hypophosphite ions,[1] which is the only source in the ENP process to provide electrons for subsequent reduction of metal ions. Consequently, copper ions cannot take up all of the reduction sites to let the autocatalytic ENP process proceed spontaneously. Otherwise, the ENP process has to cease because there is not enough supply of electrons. Therefore, some reduction sites on the plating frontier have to make room available for nickel ions. In other words, copper ions still have to compromise in harvesting the electrons against nickel ions, though they have much greater electrochemical partiality to be reduced over the nickel ions.

The initial enrichment of copper in electroless deposits is evident in Figure 10. This indicates a pure copper was indeed formed initially. Nevertheless, it does not take a long time for the copper contents in alloys to reach constant and saturated values (Figure 8). The settlement between reduction rates of cupric ions and other active species is also reflected in Figure 5, where the copper contents in deposits after being plated for 0.5 h reach certain values for each initial concentration of added cupric ions. That is, the deposition process after 0.5 h could be regarded as reaching steady-state operation. Moreover, with the initial concentration of cupric sulfate pentahydrate exceeding 200 ppm, the copper contents in the alloys plated for 30 min are nearly constant. This indicates that the availability of reduction sites on the plating frontier mediates the extents of copper deposition. Thus, a significant amount of free cupric ions still exists in the ENP bath, which is available to play a stabilizing role in the ENP bath by quickly deactivating the colloidal metal seed detached from the plating frontier. If the dimensions of these colloidal nickel particles diffused outward from the plating frontier are small enough, then, accordingly, the thickness of the electric double layer (EDL) is thinner. The barrier for the electron transfer through the EDL is lower. Consequently, cupric ions tend to be reduced on the metal particle surface in such a way as to deactivate these metal particles.

To predict the deposition rate and simultaneously to account for the initial deposition of Cu(1,1,1), the model proposed by Yin et al.[3] was revised to allow that, when the cupric concentration in the bulk is less than the critical concentration, portions of cupric ions can still reach the plating frontier at the OHP by diffusion because of the existence of a higher Cu^{2+} concentration gradient, in comparison with that of Pb^{2+}, conventionally added of less than 10 ppm, and because of a much larger reduction potential than that of Ni^{2+}, in addition to quickly settling down the Ni colloidal particles diffused outward from the OHP. With more cupric ions present in the bulk, more copper should be supposedly deposited. However, as aforementioned, reduction sites on the plating frontier have to be shared proportionally among nickel, hypophosphite, and cupric ions. Accordingly, the expression of the deposition rate of copper is analogous to that of the nickel proposed by Yin et al.[3] In the case in which the cupric concentration in the bulk, C_B^{Cu}, is less than the critical concentration, $C_B^{Cu,C}$, the deposition rates remain almost constant. Despite the fact that some portions of cupric ions could still be reduced in this case, its attribution to the overall deposition rate is practically negligible, as observed from the experimental data.

On the contrary, when $C_B^{Cu} > C_B^{Cu,C}$, the influence of the adsorbed cupric ions on the work function and the Fermi energy is considered with an introduced parameter, b. Hence, the relationship between the thermodynamic work function ϕ and the Fermi energy of the Ni−(Cu)−P layer E_f can be expressed as

$$V^0 = \phi^0 + E_f{}^0 \approx \phi + E_f + b \quad (11)$$

(20) Tachev, D.; Georgieva, J.; Armyanov, S. *Electrochim. Acta* **2001**, *47*, 359.
(21) Bard, A. J.; Faulkner, L. R. *Electrochemical Methods: Fundamentals and Applications*, 2nd ed.; John Wiley & Sons: New York, 2001.

where the superscript "0" represents conditions without the codeposited stabilizer, Cu, and V^0 is the depth of the net nuclear potential, namely, the depth of the potential well from the lowest energy state to the state of the electron being far enough outside the metal. V^0 is not necessarily a constant, and indeed, b represents the shift of the nuclear potential. It is worth mentioning that b is mainly a function of the surface concentration of adsorbed cupric ions. In this work, b is assumed to be saturated in the vicinity near the critical concentration. Accordingly, the individual rates could be revised as[3]

$$R_P = R_P{}^0 \exp[-B_1(C_B^{Cu} - C_B^{Cu,C})] \quad (12)$$

$$R_{Ni} = R_{Ni}{}^0[1 + A_1(C_B^{Cu} - C_B^{Cu,C})/(E_f{}^0 + b)]^{1/2} \exp[(16A_1 - B_1)(C_B^{Cu} - C_B^{Cu,C})] \quad (13)$$

$$R_{Cu} = k_2[E_f{}^0 + A_2(C_B^{Cu} - C_B^{Cu,C}) + b]^{1/2} \exp[(16A_2 - B_2)(C_B^{Cu} - C_B^{Cu,C}) + 16b] \quad (14)$$

where k_2 is a constant and A_i and B_i are other constants specifying the influence of adsorbed hypophosphite anions and cupric ions on the plating frontier on the work function and Fermi energy. For R_P and R_{Ni}, the constants could be obtained empirically from the deposition rates of nickel and phosphorus at any concentration $C_B^{Cu} < C_B^{Cu,C}$, i.e., 5.16 and 0.61 mg/(cm^2·h), respectively. However, with an existing discontinuity in the deposition rate of copper at the critical point, eq 14 is fitted with an approach from the larger additive concentration to the vicinity of the critical point. Moreover, the averaged deposition rate of copper is determined empirically to be 0.31 mg/(cm^2·h) with an initial concentration of $CuSO_4$·$5H_2O$ of 500 mg/L, very close to but still less than the critical value.

As aforementioned, the reduction potentials of cupric and cuprous ions are much larger than that of nickel ions. Cupric and cuprous ions can be easily adsorbed on the surface of the Ni particles through electrochemical displacement. Moreover, the work function of the pure nickel (∼5.2 eV) is decreased by the adsorbed Cu, whose work function is only about 4.6 eV.[22] The Fermi energies of nickel and copper are around 9.2 eV[23] and 7.0 eV.[22] The shift of the net nuclear potential well b could be estimated theoretically from the Fermi energy and the work function. Using the empirical information on the Ni/Cu elemental ratio of 19 found in the resulting Ni−Cu−P alloy with stabilizer added near the critical value, attributions from the work function difference and the Fermi energy difference to b are 0.03 and 0.11 eV, respectively. That is, b is projected as 0.14 eV. Coincidently, the best fit value for b is 0.12 eV in this work.

The best fits of R_P, R_{Ni}, and R_{Cu} beyond the critical concentration are described in Figure 4, from which $E_f{}^0$ is found to be about 10 eV, which is consistent with that in our previous work using Pb^{2+} as a stabilizer.[3] Furthermore, the value of $\kappa = (B_1/A_1)k_BT$ is a constant describing the influence of the work function on the adsorption tendency of $H_2PO_2^-$ anions against nickel ions.[3] The value $\kappa = 6.1$ found in this work is larger than 2.4 garnered in our previous work, indicating that the presence of cupric ions would favor the adsorption of $H_2PO_2^-$ anions. Thus, the deposition rate of the resulting EN alloy is enhanced, which is consistent with findings in the literature.[1,7,18] Moreover, the adsorbed cupric ions on the as-deposited Ni−Cu−P alloy could reduce the depth of the net nuclear potential by 0.12 eV, implying that the ionization energy is reduced. Hence, the surface free energy of the Ni−Cu−P deposits is decreased.[24] As a result, the adsorbed H_2 bubbles are more easily detached from the plating fronts during the plating process, leading to reduced formation of voids on the surface.

Interestingly, when the bulk concentration of cupric ions exceeds the critical value, the deposition rate of electroless nickel is deteriorated because of the displacement of the just-deposited nickel by the cupric ions. That is, the just-deposited Ni is consequently dissolved anodically with cupric ions into the plating bath. Finally, with initial addition of more than 3000 mg/L $CuSO_4$·$5H_2O$ in the ENP bath, the electroless copper deposition is found empirically rather than the desired electroless nickel plating.

Finally, two types of chemistry, surface and bulk, are seemingly involved in the ENP process. The surface chemistry in this work may include charge transfer, the electrochemical deposition of the substances (Ni, Cu, and P), and so on. These charge and mass transfers occur via the autocatalytic scheme, which means these transfers follow some collaborative and self-sustained steps and take place only at those surface metal sites with unsaturated coordination environments. Another important point is the passivation of colloidal Ni particles in the bulk solution that are originally detached from the as-deposited frontier.[19] However, electrochemical disproportionation of Cu^{2+} ions on these particles suppresses their autocatalytic activity. In contrast, the bulk chemistry mainly involves conventional equilibria, such as coordination equilibrium of Ni^{2+} ions with the organic chelate (e.g., citrate) that inhibits the precipitation of nickel salts of phosphite and acetate.

5. Conclusion

Addition of proper amounts of cupric ions to the plating bath significantly improves the surface morphology of the resulting electroless nickel alloys and increases the deposition rates slightly. Careful EDX analyses and concentration−depth profiles of the as-deposits are not consistent with formation of electroless Ni−Cu−P alloys. Additionally, the mass ratio of Ni/P in the as-deposit remains constant during the plating process. Instead, electroless copper appears before the electroless Ni−P alloys, and electroless nickel alloys may grow on electroless copper nuclei. Namely, copper competes with nickel for free electrons released by oxidation of hypophosphite ions on the plating frontier. The fact that copper is the preferred species is consistent with the positive reduction potential of cupric ions and the negative reduction

(22) Kittel, C. *Introduction to Solid State Physics*, 7th ed.; John Wiley & Sons: New York, 1996.
(23) Papaconstantopoulos, D. A. *Handbook of the Band Structure of Elemental Solids*; Plenum Press: New York, 1986.
(24) Adamson, A. W.; Gast, A. P. *Physical Chemistry of Surfaces*, 6th ed.; John Wiley & Sons: New York, 1997.

potential of nickel ions. The preferred facet of deposited copper is in the (1,1,1) direction. However, at a concentration of added copper sulfate pentahydrate of less than 536 mg/L, the deposition rates are not significantly altered with the presence of cupric ions owing to the limited supply of cupric ions available in the plating bath. The revised model derived from the electron tunneling theory by Yin et al.[3] has successfully predicted the deposition rates of electroless copper and Ni−P alloys. Moreover, the effect of saturated adsorbed cupric ions on the just-deposited Ni−Cu−P frontier not only enhances the adsorption of hypophosphite anions and, consequently, the deposition rates, but also shifts the depth of the net nuclear potential of the electroless nickel alloys.

Acknowledgment. This work was financially supported by the National Science Council of Taiwan. Discussion with Dr. X. Yin of the Department of Chemical and Biomolecular Engineering at the National University of Singapore is pivotal and much appreciated.

CM0527571